RSC Advances

RSC Adv

ARTICLE

C~3v~-Symmetric anion receptors with guanidine recognition motifs for ratiometric sensing of fluoride

Won Kim[a‡], Suban K Sahoo[a,b‡], Gi-Dong Kim[a], and Heung-Jin Choi[a*]

Two new tripodal receptors **3** and **4** derived from trindane framework having guanidine groups acting as hydrogen bond acceptors are synthesized and characterized for the selective recognition of anions. The anion recognition ability of the receptors was evaluated by UV-Vis absorption, fluorescence and ^{1}H NMR methods. Both the receptors showed F^{−} selective ratiometric chromogenic and fluorogenic responses among the tested anions due to the host-guest complexation followed by the abstraction of the amide-NH protons supported by the ^{1}H NMR titration study. Receptor **4** with the naphthalene fluorophore units showed high F^{−} selectively than the receptor **3** by giving visually detectable blue fluorescent and significant turn-on fluorescence at 410 nm which can be switched back and forth by successive addition of F^{−} and H^{+}. Further, the reversible and reproducible fluorescent state of **4** can be applied to design a molecular-scale sequential memory unit displaying "Write–Read–Erase–Read" functions in the form of binary logic.

Introduction

Research on anion recognition and sensing by artificial receptors have gained a burgeoning interest among the supramolecular chemists during the past decades, because of their ubiquitous nature and potential applications in various biological, industrial and environmental processes [1-8]. In general, the selective recognition of target anionic guest is a combine effect of the non-covalent interactions between the receptor (host) and guest, size-and-shape complementarity, the geometry of guest, anion basicity and the nature of the solvent etc. [9-12]. Various non-covalent interactions, such as electrostatic, anion-π, hydrogen bonding, coordinate bonding, *etc.* are used for the designing of positively charged, neutral and metal-ligand complex based anion selective receptors. Among the different approaches, neutral anion receptors containing the directional hydrogen bonding have been extensively used for the designing of receptors with specific shapes to differentiate anionic guests with different geometries and also to avoid the possible interferences by counterion during the anion recognition. Whenever these anion selective receptors are linked suitably with a chromogenic and/or fluorogenic signaling unit, the sensing of target anion can be achieved through an optical response. Recently [13-24], many anion selective optical sensors based on colorimetric and fluorescent changes have been reported to contain recognition groups, such as urea/thiourea, amide, pyrrole, sulfonamide and indole coupled with different signaling units because of the simplicity, sensitivity, low cost and online monitor of target anion without the need of expensive instrumentations.

To this library of anion selective receptors, we have introduced many tripodal anion receptors containing urea and thiourea binding sites using the rigid *C*~3v~-symmetric tripodal framework 'trindane' (**Scheme 1**) expanded either from the lower or upper feet with high recognition ability towards bioactive anions [25-28]. In the present study, we have introduced two new tripodal receptors **3** and **4** derived from trindane framework having guanidine groups acting as hydrogen bond acceptors for the selective encapsulation of anions (**Scheme 1**). The guanidine derivatives **3** and **4** are expected to behave like the reported urea based receptors with the added benefit of the conjugated aromatic systems for some optical changes for the chromogenic/fluorogenic detection of anion. The receptors are synthesized and characterized, and their anion recognition ability was evaluated by ^{1}H NMR titration, UV-Vis and fluorescence methods.
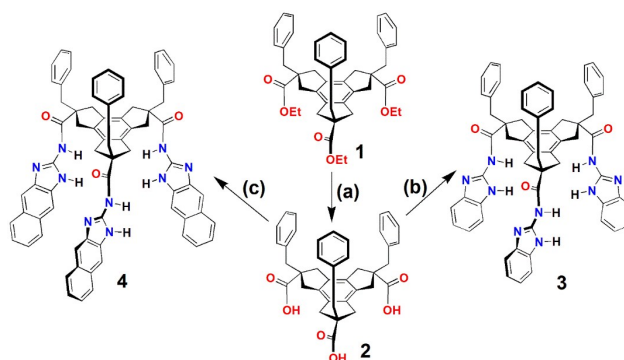
Scheme 1. Synthesis of new trindane-based *C*~3v~-symmetric anion receptors **3** and **4** with guanidine recognition motif from *cis,cis,cis*-2,5,8-tribenzyltrindane frameworks **1**: (a) THF/EtOH/H₂O (1:1:1), KOH, reflux, 12 hr; (b) i. DMA, 1,1'-carbonyldiimidazole, rt, 12 hr; ii. DMA, 2-aminobenzimidazole, 70 ºC, 18 hr; (c) i. DMA, 1,1'-carbonyldiimidazole, rt, 12 hr; ii. DMA, 1*H*-naphtho[2,3-*d*]imidazole-2-amine, 70 ºC, 18 hr.

‡*Contributed equally.*
[a] Department of Applied Chemistry, Kyungpook National University, Daegu, 702-701, South Korea. E-mail: choihj@knu.ac.kr; +82 (53) 950-5582; Fax: +82 (53) 950-6594.
[b] Department of Applied Chemistry, SV National Institute of Technology, Surat-395007, Gujrat, India.
†Electronic Supplementary Information (ESI) available: [details of any supplementary information available should be included here]. See DOI: 10.1039/x0xx00000x

Experimental

General

All chemicals and reagents of high purity were obtained commercially and were used without any further purification. DMSO (HPLC grade) was purchased from Duksan, South Korea. 1,1'-Carbonyldiimidazole, 2-aminobenzimidazole, cyanogen bromide and anhydrous N,N'-dimethylaceteamide (DMA) were purchased from Aldrich Chemical Co., USA. 2,3-Diaminonaphthalene was purchased from Alfa Aesar, USA. The solutions of anions were prepared from their tetrabutylammonium (TBA) salts of analytical grade procured from Aldrich Chemical Co., USA.

All the analytical measurements were conducted at room temperature. Column chromatography was performed on a Yamagen MPLC equipped with a fluid metering pump using Merck silica gel 60 (70-230 mesh) and CH_2Cl_2/MeOH mixed eluent. NMR spectra were recorded on a Bruker AVANCE digital 400 (400 MHz) and AVANCE III (500 MHz) spectrometer in DMSO-d_6. ^{1}H NMR and ^{13}C NMR chemical shifts are given relative to TMS. UV-Vis absorption spectra were obtained on an Optizen 2120-UV spectrophotometer. Fluorescence spectra were measured on a Shimadzu RF-5301 fluorescence spectrometer equipped with a xenon discharge lamp using 1 cm quartz cells. IR spectra were recorded on a Shimadzu IR Prestige-21 FTIR spectrometer. MALDI-TOF data were obtained on a Voyager DE-STR mass spectrometer and α-cyano-4-hydroxycinnamic acid (CHCA) was used as a matrix.

The stock solutions of host and anions (1 mM) were prepared in DMSO. These solutions were appropriately diluted further for different spectroscopic experiments to study the anion recognition and sensing ability of the hosts **3** and **4**. The spectral titrations of **3** and **4** were performed by taking 2 mL of host solution with appropriate concentration directly into cuvette and the spectra were recorded after each aliquot addition of TBAF (1 mM). All fluorescence emission spectra were recorded at a fixed excitation wavelength (λ_{ex} of receptor **3**: 299 nm and receptor **4**: 345 nm). The quantum yield (Φ) of the receptors before and after the addition of F$^-$ was calculated by applying the relationship [29]:

$$\Phi = \Phi_{ref} (I/I_{ref}) (A_{ref}/A) (\eta/\eta_{ref})^2$$

where, Φ is the radiative quantum yield of the receptor, Φ_{ref} is the quantum yield of quinine sulfate in 0.1 M aqueous H_2SO_4 (Φ_{ref} = 0.54), I is the integrated emission, A is the absorbance at the excitation wavelength, and η is the refractive index of the solvent. For ^{1}H NMR titration, the receptor solution (0.5 mL, 4.0 mM, DMSO-d_6) was taken in NMR tube and then the spectra were recorded after each stepwise addition of fluoride anion as their TBA salt prepared in DMSO-d_6.

Synthesis of *cis,cis,cis*-2,5,8-tribenzyltrindane-2,5,8-tricarboxylic acid (2)

The mixture of triethyl *cis,cis,cis*-2,5,8-tribenzyltrindane-2,5,8-tricarboxylate (70 mg, 0.11 mmol) and KOH (33 mg, 0.50 mmol) in THF (5 mL), water (5 mL) and ethanol (5 mL) medium was heated at reflux condition for 12 hours. The clear solution was concentrated under reduced pressure. The residue was acidified with conc. HCl (6 mL) and cooled in an ice bath. The precipitate was filtered and washed with 3N HCl (10 mL). The white mixture was dried. The dried mixture was taken up in THF (10 mL), and filtered to remove insoluble inorganic salt. The filtrate was concentrated and dried under high vacuum to give white solid (65 mg, 98%): **IR (KBr, cm^{-1}):** (KBr) 3062, 3027, 2924, 1702, 1201; ^{1}**H NMR** (400 MHz, DMSO-d_6) δ 12.47 (s, 3H, -CO$_2$H), 7.28 (t, J = 7.30 Hz, 6H, Ar-H), 7.21 (t, J = 7.30 Hz, 3H, Ar-H), 7.15 (d, J = 7.32 Hz, 6H, Ar-H), 3.07 (d, J = 15.6 Hz,

6H, ArCH_aH$_b$-), 2.96 (s, 6H, PhCH_2-), 2.77 (d, J = 15.6 Hz, 6H, ArCH$_a$H$_b$-); ^{13}**C NMR** (100 MHz, DMSO-d_6) δ 177.2, 138.1, 134.9, 129.5, 128.0, 126.4, 60.1, 55.0, 43.0; **MS (EI, relative intensity, m/z):** 602 (M+2, 3), 601 (M+1, 10), 600 (M+, 24), 554 (9), 509 (12), 463 (7), 417 (15), 347 (33), 191 (9), 91 (100).

Synthesis of *cis,cis,cis*-2,5,8-tribenzyl-2,5,8-tri[*N*-(1*H*-benzo[*d*]imidazol-2-yl)carbamoyl]trindane (3)

A mixture of *cis,cis,cis*-2,5,8-tribenzyltrindane-2,5,8-tricarboxylic acid (100 mg, 0.17 mmol) and 1,1'-carbonyldiimidazole (84 mg, 0.52 mmol) in anhydrous DMA (10 mL) was stirred under a nitrogen atmosphere at room temperature for 12 hours. To this, a solution of 2-aminobenzimidazole (72 mg, 0.54 mmol) in anhydrous DMA (4 mL) was added by using a syringe. The mixture was stirred further for 18 hours at 70 ºC. Then water (2 mL) was added to this reaction mixture and stirred for a while. The mixture was concentrated to dryness by vacuum distillation. The residue was purified by a column chromatography on silica gel using CH_2Cl_2 and then MeOH/CH_2Cl_2 (2:98) to give the product as a slightly yellowish solid powder (83.7 mg, 52%): **IR (KBr, cm^{-1}):** 3380 (w), 3295 (w), 3062 (w), 3032 (w), 2924 (w), 2855 (w), 1674 (m), 1628 (m), 1566 (s), 1451 (m), 1427 (m), 1273 (m), 1196 (m), 741 (s), 702 (m), 602 (w); ^{1}**H NMR (400 MHz, DMSO-d_6):** δ 12.08 (br s, 3H, N-H), 11.76 (br s, 3H, N-H), 7.51-7.39 (m, 6H, Ar-H), 7.33-7.06 (m, 21H, Ar-H), 3.32 (d, J = 15.8 Hz, 6H, ArCH_aH$_b$-), 3.28 (s, 6H, ArCH_2), 3.08 (d, J = 15.8 Hz, 6H, ArCH_aH$_b$-); ^{13}**C NMR (100 MHz, DMSO-d_6):** δ 176.5 (br), 148.1 (br), 141.4, 138.9, 135.9, 133.4 (br), 130.4, 129.2, 127.5, 122.1, 117.8 (br), 112.6 (br), 58.0, 43.6 (br), 40 (overlapped with DMSO-d_6), referenced to *cis,cis,cis*-2,5,8-tribenzyl-2,5,8-tri(carbamoyl)trindane (δ 178.3, 139.3, 135.9, 130.3, 128.4, 126.6, 56.4, 44.0, 40.2); **MALDI-TOF-MS, *m/z* (rel intensity):** 946.7956 (100), 947.7957 (74), 948.7990 (23), Calcd for $C_{60}H_{51}N_9O_3$: *m/z* 946.4193 (M + H$^+$, 100), 947.4227 (68.2), 948.4260 (22.9).

Synthesis of *cis,cis,cis*-2,5,8-tribenzyl-2,5,8-tri[*N*-(1*H*-naphtho[2,3-*d*]imidazol-2-yl)carbamoyl]trindane (4)

Synthesis of 1H-naphtho[2,3-d]imidazol-2-amine [30]: In a 100 mL round bottom flask, 2,3-diaminonaphthalene (158 mg, 1 mmol) was dissolved in a mixture of MeOH/water (1:1, 20 mL). The reaction mixture was treated with cyanogen bromide (165 mg, 1.55 mmol) and heated at 50 ºC for 1 hour. After cooling to room temperature, the solvent was removed in vacuo, and the residue was basified with 1 M KOH (to pH 10) and extracted with EtOAc (30 mL X 3). The combined organic fractions were dried with MgSO$_4$, filtered and concentrated in vacuo. The reaction mixture was purified by recrystallization from *n*-hexane/THF to yield greenish brown powder (180 mg, 98%): ^{1}H NMR (400 MHz, DMSO-d_6) δ 10.88 (br s, 1H, N-H), 7.81 (m, 2H, Ar-H), 7.51 (s, 2H, Ar-H), 7.25 (m, 2H, Ar-H), 6.67 (br s, 2H, -NH$_2$).

Synthesis of trindane receptor 4: A mixture of *cis,cis,cis*-2,5,8-tribenzyltrindane-2,5,8-tricarboxylic acid (100 mg, 0.17 mmol) and 1,1'-carbonyldiimidazole (84 mg, 0.52 mmol) in anhydrous DMA (10 mL) was stirred under a nitrogen atmosphere at room temperature for 12 hours. To this solution was added a solution of 1*H*-naphtho[2,3-*d*]imidazole-2-amine (100 mg, 0.54 mmol) in anhydrous DMA (5 mL) *via* a syringe. The mixture was stirred further for 18 hours at 70 ºC. After cooling to room temperature, to this reaction mixture was added water (5 mL) and stirred for a while. The mixture was concentrated by vacuum distillation. The residue was purified by a column chromatography on silica gel using CH_2Cl_2 and then MeOH/CH_2Cl_2 (2:98) to give the product (97 mg, 52%): **IR (KBr, cm^{-1}):** 3378 (m), 3055 (w), 2921 (w), 2847 (w), 1677 (m), 1648 (m), 1567 (s), 1504 (m), 1424 (s), 1263 (m), 1160 (m), 858 (m), 732 (m), 700 (m); ^{1}**H NMR (400 MHz, DMSO-d_6):** δ 12.17 (br s,

Please do not adjust margins

3H, N-H), 12.02 (br s, 3H, N-H), 8.04-7.75 (m, 12H, Ar-H), 7.40-7.16 (m, 21H, Ar-H), 3.37 (d, J = 14.6 Hz, 6H, ArCH_aH_b-), 3.32 (s, 6H, ArCH_2), 3.10 (d, J = 14.6 Hz, 6H, ArCH_aH_b-); **^{13}C NMR (100 MHz, DMSO-d_6):** δ 176.8 (br), 151.7 (br), 139.0, 135.9, 130.4, 129.1, 128.4, 127.4, 124.0, 113.1 (br), 107.6 (br), 58.3, 43.5 (br), 41.4 (overlapped with DMSO-d_6); **MALDI-TOF-MS, m/z (rel intensity):** 1096.7208 (100), 1097.7255 (86), 1098.7271 (36), 1099.7305 (10), Calcd for $C_{60}H_{51}N_9O_3$: m/z 1096.4663 (M + H^{+}, 100), 1097.4696 (81.2), 1098.4730 (32.5), 1099.4763 (7.5).

Results and discussion

The synthesis of receptors **3** and **4** were achieved by following the steps shown in **Scheme 1** and characterized by various spectral techniques before embarking for further anion recognition and sensing. The trindane tricarboxylic ester scaffold (**1**) which was used as a starting material of trindane tricarboxylic acid (**2**) was synthesized from mesitylene in seven steps by following our reported methods with an overall yield of 10 % (Scheme S1) [26]. The trindane tricarboxylic acid **2** was synthesized in 98% yield from hydrolysis of trindane tricarboxylic ester **1** with potassium hydroxide in THF/ethanol/water (1:1:1) medium at reflux condition. Anion receptor **3** was synthesized from the reaction of **2** and 2-aminobenzimidazole *via* carbonyl activation with carbonyldiimidazole in 52% yield. Receptor **3** was purified by a column chromatography to remove of excess of 2-aminobenzimidazole and mono/di-substituted compounds. Similarly, anion receptor **4** with naphthoimidazole recognition motif was synthesized and purified by a column chromatography to remove the excess of starting reagent and mono/di-substituted compounds. Both the receptors are soluble in common organic solvents such as DMSO, THF, CH_2Cl_2, CH_3CN, but insoluble in water. The molecular structure of receptors **3** and **4** were characterized by various spectral (IR, ^{1}H NMR, ^{13}C NMR) and MALDI-TOF (Fig. S1a-S2a) data. The ^{1}H NMR spectrum of **3** showed two peaks at δ 12.08 and 11.76 ppm attributed to the imidazole-NH and amide-NH protons, respectively (Fig. S1b). The C_{3v}-symmetrical form of **3** was ascertained from the appearance of two sets of doublets (δ 3.32 and 3.08 ppm, [2]J = 15.8 Hz) for the two diastereotopic benzylic protons and a singlet at δ 3.28 ppm for the methylene protons of benzyl groups. Similarly, the imidazole-NH and amide-NH protons peaks of receptor **4** were appeared at δ 12.17 and 12.02 ppm, respectively (Fig. S2b). Also, the two diastereotopic benzylic protons showed two sets of doublets (δ 3.37 and 3.10 ppm, [2]J = 14.6 Hz) and a singlet appeared at δ 3.32 ppm for the methylene protons of benzyl groups that supported the C_{3v}-symmetrical structure of receptor **4**.

The anion recognition and sensing ability of the receptors **3** and **4** towards F[-], Cl^{-}, Br^{-}, HSO_4^-, $H_2PO_4^-$, NO_3^-, $CH_3SO_3^-$ and $C_7H_7SO_3^-$ anions was investigated by the ^{1}H NMR, colorimetric and fluorometric methods in DMSO. As shown in Fig. 1a-b, the receptor **3** showed absorption bands at 265, 290 and 299 nm, whereas **4** at 265, 331, 338 and 345 nm due to multiple π-π* transitions. Upon addition of F[-], the absorption bands of **3** and **4** were selectively red-shifted to 320 nm and 372 nm, respectively. The appearance new red-shifted band indicates the formation of an anion-receptor complex through intramolecular hydrogen bonds and/or the strong basicity of F[-] triggered the abstraction of –NH protons which accelerated the internal charge transfer (ICT) between the receptor and added F[-]. No noticeable spectral changes of the receptors **3** and **4** were observed with other tested anions. Also, the F[-]-induced spectral changes of the receptors were not interfered under competitive environment. The UV-Vis absorption titration of

receptors **3** and **4** (10 μM) was next performed by the incremental addition of TBAF from 1 to 100 equivalents (Fig. 1c-d) to determine the anion binding constant. Addition of just 1 equivalent of F[-] *i.e.* 10 μM to the receptors **3** and **4** solutions resulted the appearance of the new charge-transfer band at 320 nm and 372 nm, respectively. With the further addition of F[-], the intensity of the charge transfer band attributed to new receptor-anion complex species formed in solution was enhanced continuously with the formation of isosbestic points at 300 nm for **3**, and at 271 and 340 nm for **4**. The spectral changes shown by the receptors clear indicate the similar F[-] recognition modes. Analysis of the UV-Vis titration data with the least-square fitting equation [31] showed best fit for 1:1 binding stoichiometry with the binding constant of 4.5×10^3 M^{-1} and 6.5×10^3 M^{-1} for **3**.F[-] and **4**.F[-], respectively (Fig. S3). The higher F[-] binding ability of receptor **4** can be linked with the enhanced aromatic platform due to the naphthalene group that generated a more preorganized deep hollow cavity to accommodate fluoride ions.
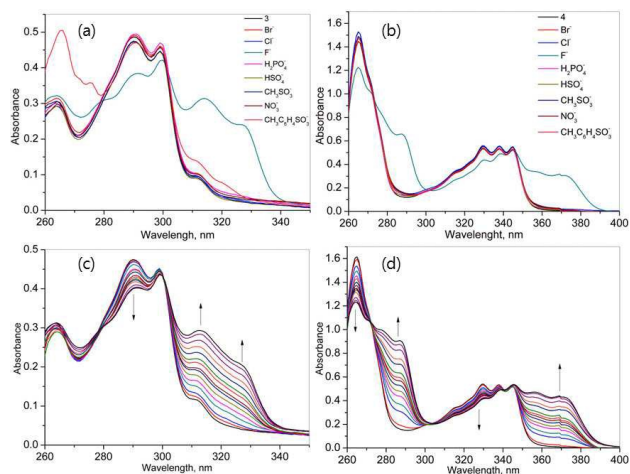

Fig. 1. Changes in the UV–Vis absorption spectra of receptors (10 μM) **3** (a) and **4** (b) in absence and presence of 100 equiv of selected anions in DMSO. The UV–Vis spectral changes of **3** (c) and **4** (d) upon incremental addition of TBAF from 1, 2, 3, 5, 7, 10, 13, 16, 20, 30, 40, 60, 80 to100 equiv.

The fluoride recognition behavior of the receptors was examined by recording the ^{1}H NMR spectra of the receptors **3** (Fig. 2) and **4** (Fig. S4) after adding different equivalents of F[-]. Upon addition of 0.5 equivalent of F[-], the imidazole-NH and amide-NH protons (H_b) peaks at δ 12.08 and 11.76 ppm were broadened significantly due to the possible hydrogen bonding interactions occurred between **3** and F[-]. At higher equivalents of F[-], the amide-NH protons peak disappeared completely and a new peak appeared at 15.5 ppm for the formation of bifluoride ions *i.e.* HF_2^- [32]. Other peaks, including the characteristic peaks due to the C_{3v}-symmetry of **3** were not shifted throughout the titrations. The receptor **4** also showed similar changes in ^{1}H NMR titration experiment with TBAF (Fig. S4). Therefore, it can be proposed that the receptors first forming the hydrogen bonded host-guest complex with F[-] and then the deprotonation of most acidic amide-NH protons occurred when F[-] added in excess.

The anion recognition ability of the receptors **3** and **4** was next investigated by fluorescence spectroscopy in DMSO. The receptor **3** (10 μM) showed a weak fluorescence at 328 nm (Φ = 0.003), when excited at 299 nm (Fig. S5). Addition of F[-] in excess (100 equiv.) caused a slight red-shift in fluorescence band from 328 nm to 336

nm (Φ = 0.004). With naphthalene fluorophore, the receptor **4** (5 µM) showed a broad fluorescence between 350 nm to 450 nm with emission maxima at 368 nm (Φ = 0.004). Upon addition of 50 equiv of F$^-$ resulted quenching in the fluorescence of the receptor **4** and a new fluorescence band was appeared in the visible region with emission maxima at 410 nm (Φ = 0.01) (Fig. 3). The ratiometric fluorescence response of **4** is highly selective and specific, occurred only in the presence of F$^-$, and not interfered in the presence of other competing anions. In addition, a selective naked-eye detectable fluorescent color change of **4** was observed upon addition of F$^-$ (inset Fig. 3).
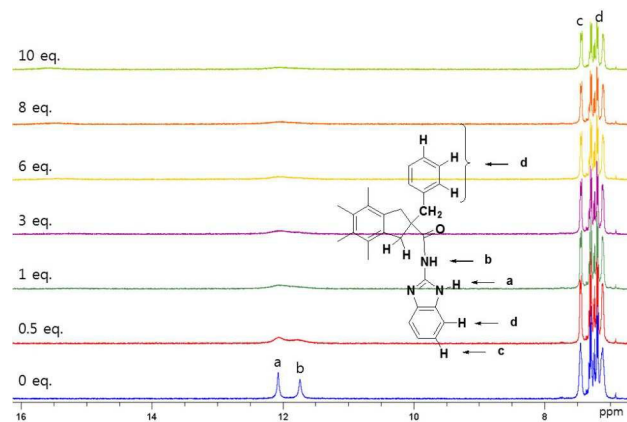

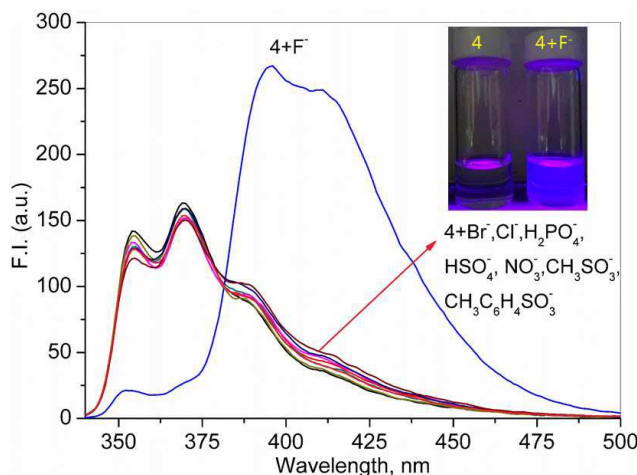**Fig. 2.** Partial ^{1}H NMR spectral changes of **3** (4 mM) upon addition of TBAF in DMSO-d_6.

Fig. 3. Changes in the fluorescence spectra of receptor **4** (5 µM) after addition of 50 equiv of selected anions in DMSO (λ_{ex} = 345 nm). Inset shown a color change of vials under UV light (365 nm).

The fluorescence titration of **4** was performed by the incremental addition of TBAF in DMSO (Fig. 4). The typical naphthalene fluorescence of **4** decreases gradually and the emission at 410 nm was appeared with the formation of a well-defined isoemission point at 378 nm. The structural modification of **4** at the excited state upon addition of F$^-$ that led to the significant enhancement of fluorescence at 410 nm was most likely due to the hydrogen bonding interactions to the polar-NH groups followed by the deprotonation of most acidic amide-NH protons. It is worthy to mention here that fluoride binding resulted fluorescence turn-off for most of the reported sensors with only a few exhibiting

fluorescence turn-on [33]. Further to complement the proposed deprotonation mechanism, the fluorescence spectra of **4** was recorded in the presence of strong base NaOH that showed similar turn-on fluorescence at 410 nm as observed with TBAF (Fig. S6). Further, the fluorescence of receptor **4** was reversed back upon subsequent addition of HCl.
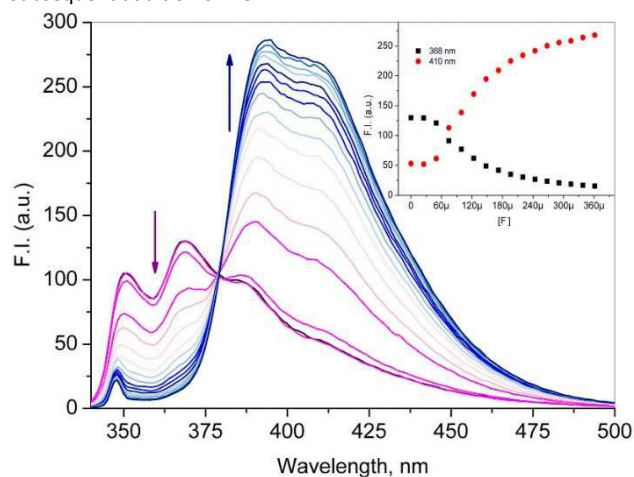

Fig. 4. The fluorescence spectral changes of **4** (5µM) upon incremental addition of TBAF in DMSO. Inset showing the change in fluorescence intensity of **4** at 368 nm and 410 nm at different concentration of TBAF.

The 'Off-On' fluorescent state of **4** and increase in the emission intensity ratio *i.e.* I$_{410}$/I$_{368}$ with the increase in the [F$^-$] linearly from 49.8 µM to 361 µM indicates the possible application of **4** for the ratiometric fluorescent sensing of F$^-$ ions. Using the fluorescence titration data, the F$^-$ detection limit of 208 nM was estimated using the slope of the calibration curve (Fig. S7) and the equation 3σ/slope (where σ represents the standard deviation of the blank). The United States Environmental Protection Agency (USEPA) mandates a drinking water standard for F$^-$ of 100 µM and 200 µM respectively to prevent dental fluorosis and osteofluorosis [34], but a recent review demonstrated that the intake of F$^-$ above 250 µM can caused bone damage and mottled teeth [35]. The estimated detection limit of **4** for the ratiometric detection of F$^-$ supported its analytical novelty.

Anion recognition and sensing in protic solvents, such as water, ethanol is challenging because of the competing nature with anions for the receptor binding sites that disturbed the hydrogen bonding interactions between the receptor and the anionic guest [36]. Among the various anions, the F$^-$ is known to show high hydration energy due to the considerably high bond strength (569 kJ/mol) of its conjugated acid (HF) and therefore its detection from aqueous medium is very challenging. In order to detect F$^-$ from aqueous medium, the fluorescence spectra of **4** were recorded in the presence of 50 equiv of F$^-$ in DMSO containing different percentages of water (Fig. S8). We have observed that the F$^-$-induced turn-on fluorescence at 410 nm can be observed distinguishably in DMSO containing water not more than 7.5%. The fluorescence titration of **4** was next performed at the optimized condition of DMSO:H$_2$O (95:5, *v/v*). As shown in Fig. 5, the incremental addition of F$^-$ resulted fluorescence enhancement at 390 and 410 nm linearly from 123 µM to 909 µM and concomitantly quenched at 368 nm with the formation of an isoemission point at 378 nm.

ARTICLE

As discussed above, the receptor **4** showed an instantaneous color change under UV light along with a drastic red-shift in the fluorescence from 368 nm to 410 nm in DMSO upon F⁻ binding. The F⁻-induced fluorogenic process of **4** was reversed with the addition of H⁺, results in disappearance of the **4**.F⁻ emission bands at 410 nm and reappearance of the fluorescence at 368 nm. Especially, the reversible fluorescence changes could be repeated for several times by alternating addition of F⁻ and H⁺ (Fig. 6), mimicking the behavior of an optical switch.
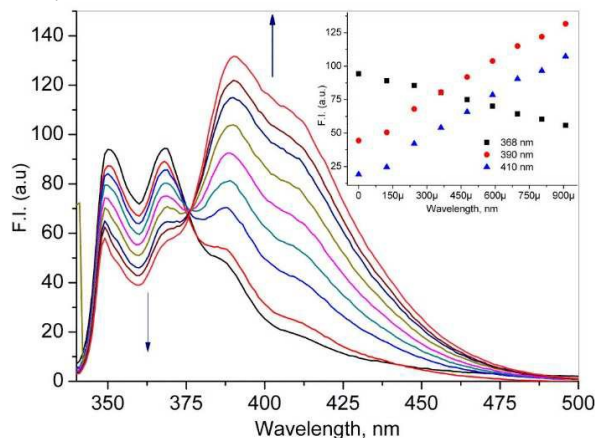

Fig. 5. The fluorescence spectral changes of **4** (5 µM) upon incremental addition of TBAF in DMSO containing 5% H_2O. Inset showing the change in fluorescence intensity of **4** at 368 nm, 390 nm and 410 nm at different concentration of TBAF.

Optical switches have great interest for molecular-level information processing and for the designing of Boolean type logic gates at the molecular level [37-39]. As depicted in Fig. 7a-b, the fluorescence switching process of **4** may be represented by a molecular "INHIBIT/IMPLICATION" type logic gates by employing F⁻ (Inp1) and H⁺ (Inp2) as the chemical inputs and the fluorescence intensity at 410 nm and 368 nm as the outputs. When the fluorescence at 368 nm was used as output, an "IMPLICATION" (a combination of NOT and OR logic gates) logic gate can be fabricated. However, an "INHIBIT" (a combination of AND and NOT logic gates) logic gate can be constructed if the fluorescence at 410 nm was used as an output. In this way, a complementary IMP/INH logic functions can be realized based on the fluorescence switching of receptor **4**. Overall, the fluorescent changes of **4** in DMSO are controlled by the chemical inputs of F⁻ and H⁺: F⁻ switches ON the optical output, while H⁺ switches OFF the optical output.

The reversible and reproducible fluorescence switching process of **4** can also be used to design a useful sequential logic circuit displaying "Write-Read-Erase-Read" behavior in the form of binary logic for molecular-level information processing (Fig. 7c-d). The ON state (Output 2 = 1) is defined as the strong fluorescence at 410 nm, whereas the OFF state (Output 2 = 0) corresponds to the significantly weak fluorescence at 410 nm. The inputs are constituted by F⁻ (Inp1) and H⁺ (Inp2) for the 'set' and 'reset', respectively. The operation of this memory unit is as follows: whenever the set input is high (S = 1), the system writes and memorizes the binary state 1; on the other hand, when the reset input is high (R = 1), the 1 state is erased and the 0 state is written and memorized. The reversible and reconfigurable sequences of fluorescence output at λ_{em} = 410 nm for the set/reset logic operations in the feedback loop demonstrated the memory feature with "Write-Read-Erase-Read" functions. Also, the "ON–OFF" states

of **4** could be repeated for many times, suggesting "Write-Read-Erase-Read" cycles could be conducted. In other words, this system exhibits "Multi-write" ability without obvious degradation in its optical output at 410 nm.
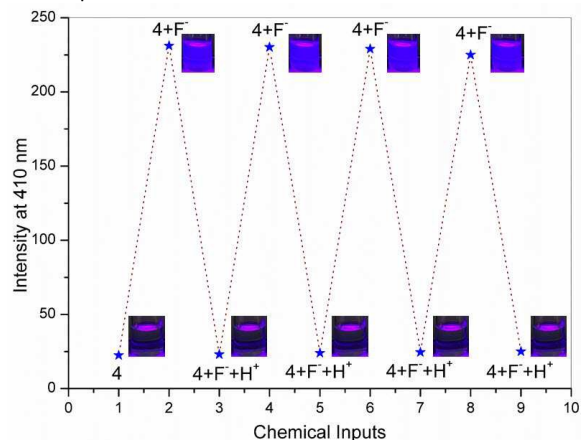

Fig. 6. Change in fluorescence intensity of **4** (5 µM) upon an alternate addition of F⁻ and H⁺ in DMSO (λ_{ex}= 345 nm).
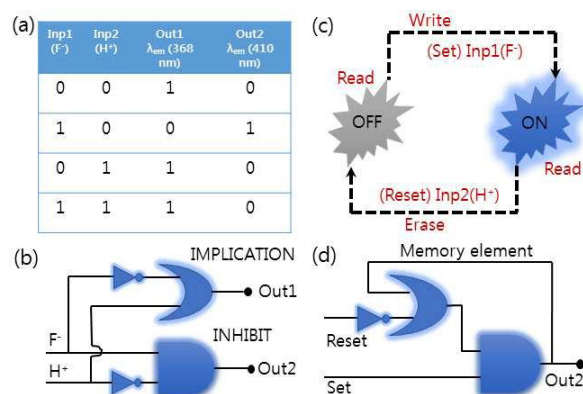

Fig. 7. The (a) truth table and (b) logic gates for the IMPLICATION and INHIBIT logic gates. (c) Feedback loop showing reversible logic operations mimicking "Read-Erase-Write-Read" functions and (d) the sequential logic circuit for memory element with two inputs and one output.

The quantum mechanically calculated structure of the receptors **3** and **4**, and their host-guest complexes with F⁻ was obtained through density functional theory (DFT) method. The equilibrium conformers of the receptors and their F⁻ complexes were first searched by applying the MMFF force field and the computational program Spartan'14. The least strain structure obtained by the conformational search was next optimized by the DFT method at B3LYP/6-31G* level in the gas phase. As shown in Fig. 8, the three appended arms of the receptors were oriented in the same direction to maintain the C_{3v}-symmetry with the help of multiple intramolecular/intrastand hydrogen bonding which gave a perfect geometry to accommodate incoming anionic guest within the cavity. Compare to **3**, the receptor **4** with longer aromatic platform showed better tripodal symmetry with a deep hollow cavity that resulted higher binding ability towards F⁻. Similar to urea-based tripodal anion receptors, the F⁻ was encapsulated within the cavity of the receptors to form 1:1 caviplex by forming six hydrogen bonds with the imidazole-NH and amide-NH groups. The calculated average bond lengths for the amide-NH⸱⸱⸱F⁻ and imidazole-NH⸱⸱⸱F⁻

bonds in **3**•F⁻ complex were 2.135 Å and 1.678 Å, whereas of 2.286 Å and 1.669 Å in **4**•F⁻ complex, respectively.
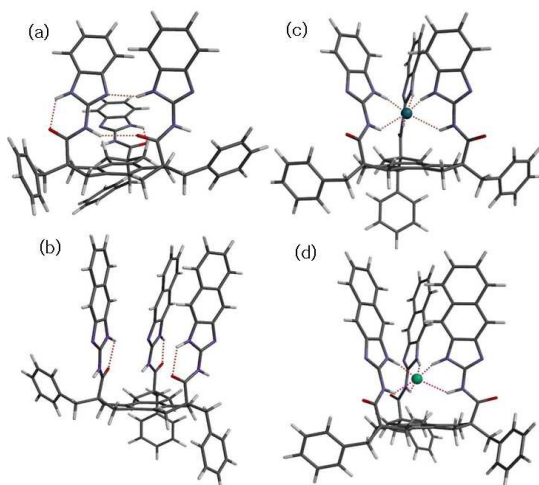

Fig. 8. The DFT computed (B3LYP/6-31G*) structure of (a) receptor **3**, (b) receptor **4**, (c) **3**•F⁻ and **4**•F⁻.

Conclusions

In conclusion, we have introduced two new C_{3v}-symmetrical receptors **3** and **4** with guanidine recognition motif for the selective recognition and sensing of bioactive anions. The UV-Vis absorption and fluorescence spectra recorded for the receptors **3** and **4** showed selectivity towards fluoride due to the selective formation of hydrogen bonded host-guest complex followed by the deprotonation of amide-NH protons. The spectral changes were depends on the substituent used. In compared to **3**, the receptor with naphthoimidazole group showed 40 nm red-shift in the UV-Vis spectral study and a significant fluorescence enhancement at 410 nm in the presence of fluoride. The receptor **4** also showed a F⁻-induced visually detectable color change under UV light and potential to detect F⁻ ratiometrically with the detection limit down to 208 nM. The fluorescence changes triggered by F⁻ cab be reversed with the addition of H⁺, which allowed to construct different logic gates and sequential logic operations mimicking "Read-Erase-Write-Read" functions at the molecular level.

Notes and references

1. J.-M. Lehn, Supramolecular Chemistry, VCH, Weinheim, 1995.
2. Supramolecular Chemistry of Anions (Eds.: A. Bianchi, K. Bowman-James, E. Garcia-Espana), Wiley-VCH, New York, USA, 1997.
3. J.L. Sessler, P.A. Gale, W.-S. Cho, in Anion Receptor Chemistry, ed. J. F. Stoddart, Monographs in Supramolecular Chemistry, Royal Society of Chemistry, Cambridge, 2006.
4. J.L. Atwood, J.W. Steed, Encyclopedia of Supramolecular Chemistry, Marcel Dekker, New York, 2004.
5. N.H. Evans, P.D. Beer, *Angew. Chem. Int. Ed.*, 2014, **53** , 11716–11754.
6. P.A. Gale, *Chem. Comm.*, 2011, **47**, 82-86.
7. R.M. Duke, E.B. Veale, F.M. Pfeffer, P.E. Kruger, T. Gunnlaugsson, *Chem. Soc. Rev.*, 2010, **39**, 3936-3953.
8. Y. Zhou, J.F. Zhang, J. Yoon, *Chem. Rev.*, 2014, **114**, 5511–5571
9. D.G. Cho, J.L. Sessler, *Chem. Soc. Rev.*, 2009, **38**, 1647-1662.
10. H.T. Ngo, X. Liu, K.A. Jolliffe, *Chem. Soc. Rev.*, 2012, **41**, 4928-4965.
11. M.E. Moragues, R. Martinez-Manez, F. Sancenon, *Chem. Soc. Rev.*, 2011, **40**, 2593-2643.
12. P.A. Gale, N. Busschaert, C.J. Haynes, L.E. Karagiannidis, I.L. Kirby, *Chem. Soc. Rev.*, 2014, **43**, 205-241.
13. C. Caltagirone, P.A. Gale, *Chem. Soc. Rev.*, 2009, **38**, 520-563.
14. P.A. Gale, *Chem. Soc. Rev.*, 2010, **39**, 3746-3771.
15. M. Wenzel, J.R. Hiscock, P.A. Gale, *Chem. Soc. Rev.*, 2012, **41**, 480-520.
16. C. B. Rosen, D. J. Hansen, K. V. Gothelf, *Org. Biomol. Chem.*, 2013, **11**, 7916-7922.
17. Z. Xu, X. Chen, H.N. Kim, J. Yoon, *Chem. Soc. Rev.*, 2010, **39**, 127-137.
18. M. Cametti, K. Rissanen, *Chem. Comm.*, 2009, 2809-2829.
19. L. Xu, Y. Li, Y. Yu, T. Liu, S. Cheng, H. Liu, Y. Li, *Org. Biomol. Chem.*, 2012, **10**, 4375-4380.
20. X. Yong, M. Su, W. Wang, Y. Yan, J. Qu, R. Liu, *Org. Biomol. Chem.*, 2013, **11**, 2254-2257.
21. L. Gai, J. Mack, H. Lu, T. Nyokong, Z. Li, N. Kobayashi, Z. Shen, *Coord. Chem. Rev.*, 2015, **285**, 24-51.
22. D. Sharma, S. K. Sahoo, S. Chaudhary, R. K. Bera, J. F. Callan, *Analyst*, 2013, **138**, 3646-3650.
23. D. Sharma, A. Moirangthem, S. K. Sahoo, A. Basu, S. M. Roy, R. K. Pati, S.K. Ashok Kumar, J. P. Nandre, U. D. Patil, *RSC Adv.*, 2014, **4**, 41446-41452.
24. D. Sharma, A. Moirangthem, R. Kumar, S. K. Ashok Kumar, A. Kuwar, J. F. Callan, A. Basu, S. K. Sahoo, *RSC Adv.*, 2015, **5**, 50741-50746.
25. W. Kim, S. K. Sahoo, G.-D. Kim, H.-J. Choi, *Tetrahedron*, 2015, **71**, 8111-8116.
26. H.-J. Choi, Y.S. Park, S.H. Yun, H.-S. Kim, C.S. Cho, K. Ko, K.H. Ahn, *Org. Lett.*, 2002, **4**, 795-798.
27. Y.S. Park, S.-H. Bang, H.-J. Choi, *Tetrahedron Lett.,* 2013, **54**, 6708-6711.
28. Y.S. Park, W. Kim, H.-J. Choi, *Bull. Korean Chem. Soc.*, 2014, **35**, 3343-3345.
29. R. Akbar, M. Baral, B.K. Kanungo, *J. Photochem. Photobiol. A*, 2014, **287**, 49-64.
30. F. Reto, S.B. Anthony, E.B. Helen, *Angew. Chem. Int. Ed.*, 2012, **51**, 5226-5229.
31. B. Valeur, J. Pouget, J. Bourson, M. Kaschke, N.P. Ernsting, *J. Phys. Chem.* 1992, **96**, 6545-6549.
32. J.-O. Park, S.K. Sahoo, H.-J. Choi, *Spectrochim Acta A*, 2016, **153**, 199-205
33. Q. Lin, Q.-P. Yang, B. Sun, J.-C. Lou, T.-B. Wei, Y.-M. Zhang, *RSC Adv.*, 2015, **5**, 11786-11790.
34. J. Fawell, K. Bailey, J. Chilton, E. Dahi, L. Fewtrell, Y. Magara, Fluoride in Drinking Water, WHO Drinking-Water Quality Series, IWA Publishing, London, UK, Seattle, USA, 2006.
35. P.T. Harrison, *J. Fluorine Chem.*, 2005, **126**, 1448-1456.
36. D. Sharma, A. R. Mistry, R. K. Bera, S. K. Sahoo, *Supramolecular Chem.*, 2013, **25**, 212-220.
37. A.P. De Silva, H.Q.N. Gunaratne, C.P. McCoy, A.P. De Silva, H.Q.N. Gunaratne, C.P. McCoy, *Nature*, 1993, 364, 42-44.
38. B. Kumar, M.A. Kaloo, A.R. Sekhar, J. Sankar, *Dalton Trans.*, 2014, **43**, 16164–16168.

39. S. Erdemir, O. Kocyigit, *Sensors and Actuators B*, 2015, **221**, 900–905.

Please do not adjust margins

Graphical Abstract